

Spectral rate theory for two-state kinetics

Jan-Hendrik Prinz, John D. Chodera, and Frank Noé

Classical rate theories fail in cases where the observable(s) or order parameter(s) used are poor reaction coordinates and no clear separation between reactants and products is possible. Here, we present a general rate theory for ergodic dynamical systems in thermal equilibrium that explicitly takes into account how the system is observed. The theory allows the systematic estimation errors made by standard rate theories to be understood and quantified. We also elucidate the connection of spectral rate theory with the popular Markov state modeling (MSM) approach for molecular simulation studies. An optimal rate estimator is formulated that gives robust and unbiased results even for poor reaction coordinates and can be applied to both computer simulations and single-molecule experiments. No definition of a dividing surface is required, and a measure of the reaction coordinate quality (RCQ) becomes readily available. Additionally, the respective projected probability distributions can be obtained for the reactant and product states along the observed order parameter, even when these strongly overlap. The approach is demonstrated on numerical examples and experimental single-molecule force probe data, here focusing on the case of two-state kinetics.

PACS numbers:

Keywords:

The description of complex molecular motion through simple kinetic rate theories has been a central concern of statistical physics. A common approach, first-order rate theory, treats the relaxation kinetics among distinct regions of configuration space by single-exponential relaxation. There has been a recent interest in estimating such rates from fluctuation trajectories of single molecules, resulting from the recent maturation of measurement techniques that are able to collect extensive traces of single molecule extensions or fluorescence [12, 15]. When the available observable or order parameter is a good reaction coordinate that allows the slowly-converting states to be clearly separated (see Fig 1 top left), classical rate theories apply and the robust estimation of transition rates is straightforward using a variety of means [32]. However, in the common case in which the reaction coordinate is poor and the separation of the slowly-converting states is not obvious, a satisfactory theoretical description is missing and many estimators break down.

Most rate theories and estimators are based upon dividing the observed state space into a reactant and a product substate and then in some way counting transition events that cross the dividing surface. Transition state theory measures the instantaneous flux across this surface, which is known to overestimate the rate due to the counting of unproductive recrossings over the dividing surface on short timescales [10]. Reactive flux theory [3] has proposed to cope with this by counting a transition event only if it has succeeded to stay on the product side after a sufficiently long lag time τ . Reactive flux theory involves derivatives of autocorrelation functions that are numerically unreliable to evaluate [7]. In practice, one therefore typically estimates the relaxation rate *via* an exponential fit to the tail of a suitable correlation function, such as the number correlation function of reactants or the autocorrelation function of the experimen-

tally measured signal [9, 29, 32]. In order to transform this relaxation rate into a forward and backward rate constant, a clear definition of reactant and product is needed, requiring that they are separable in the available observable.

Markov models (MSMs) have recently become a popular approach to producing a simplified statistical model of complex molecular dynamics from molecular simulations and can be regarded as an attempt towards a multistate rate theory. MSMs use a transition matrix describing the probability a system initially found in a substate i is found in substate j a lag time τ later. When the state division allows the metastable states of the system to be distinguished [4, 5, 20, 24], the transition matrix with a sufficiently large choice of τ can be used to derive a phenomenological transition rate matrix that accurately describes the interstate dynamics [30]. This is explicitly done for the two-state case in [7]. It has been shown in [24, 26] that by increasing the number of substates used to partition state space, and hence using multiple dividing surfaces instead of a single one, these rate estimates become more precise. In the limit of infinitely many substates, the eigenfunctions of the dynamical propagator in full phase space are exactly recovered, and the rate estimates become exact even for $\tau \rightarrow 0^+$ [14]. In practice, however, a finite choice of τ is necessary in order to have a small systematic estimation error, especially if “uninteresting” degrees of freedom such as momenta or solvent coordinates are discarded. An alternative way of estimating transition rates is by using a state definition that is incomplete and treats the transition region implicitly *via* committor functions that may better approximate the eigenfunctions of the dynamical propagator in this region [2, 28].

The quality of the rate estimates in all of the above approaches relies on the ability to separate the slowly-

converting states in terms of some dividing surface or state definition. The above approaches break down in the case where the available observables or order parameter(s) do not permit such a separation, i.e. when kinetically distinct states overlap in the histogram of the observed order parameter. However, such a scenario may often arise in single-molecule experiments where the available order parameter depends on what is experimentally observable and may not necessarily be a good reaction coordinate. In principle, Hidden Markov Models (HMMs) are able to estimate transition rates even in such situations [6, 11, 13, 16]. However, HMMs need a probability model of the measurement process to be defined, they are relatively complex to handle and implement, and they represent a machine learning approach rather than a physical theory.

Here, we present a general rate theory for stochastic dynamics that are observed on a possibly poor reaction coordinate. It is assumed that the dynamical law governing evolution of the system is a time-stationary Markov process in full-dimensional phase space, obeys microscopic detailed balance, and supports a unique stationary distribution—criteria satisfied for many physical systems of interest. These dynamics are then projected onto some observable in which they are no longer Markovian and may not easily be separable by a simple dividing surface. This framework allows us to (i) evaluate the quality of existing estimators and propose optimal estimators for the slowest relaxation rate, (ii) provide an absolute measure of reaction coordinate quality (RCQ), and (iii) derive an optimal estimator for the probabilities of and transition rates between the slowly converting states, even if these strongly overlap in the observation.

The present rate theory is exclusively concerned with the systematic error in estimating rates and proposes “optimal” methods that minimize this systematic rate estimation error. Therefore all statements are strictly valid only in the data-rich regime. Explicit treatment of the statistical error in the data-poor regime is beyond the scope of the present work but discussed at the end of the paper.

Full-space dynamics

We consider a dynamical system that follows a stationary and time-continuous Markov process \mathbf{x}_t in a generally large and continuous state space Ω . \mathbf{x}_t is assumed to be ergodic with a unique stationary density $\mu(\mathbf{x})$. In order to be independent of specific dynamical models we use the general transition density $p_\tau(\mathbf{x}_t, \mathbf{x}_{t+\tau})$, i.e. the probability density that given the system is at point $\mathbf{x}_t \in \Omega$ at time t , it will be found at point $\mathbf{x}_{t+\tau} \in \Omega$ a lag time τ later. We will at this point also assume that the dynamics obey microscopic detailed balance, i.e. $\mu(\mathbf{x}_t) p_\tau(\mathbf{x}_t, \mathbf{x}_{t+\tau}) = \mu(\mathbf{x}_{t+\tau}) p_\tau(\mathbf{x}_{t+\tau}, \mathbf{x}_t)$, which is true

for systems that are not driven by external forces. In this case, $\mu(\mathbf{x})$ is a Boltzmann distribution in terms of the system’s Hamiltonian. The following rate theory can also be formulated for some nonreversible dynamics, but the notation becomes more involved and the quantities are more difficult to interpret; we therefore restrict our discussion to the reversible case here.

The transition density can be expanded into relaxation processes that are associated with different intrinsic rates by developing it in terms of the eigenvalues and eigenfunctions of the corresponding transfer operator [24, 26]:

$$p_\tau(\mathbf{x}_t, \mathbf{x}_{t+\tau}) = \sum_{i=1}^{\infty} e^{-\kappa_i \tau} \psi_i(\mathbf{x}_t) \mu(\mathbf{x}_{t+\tau}) \psi_i(\mathbf{x}_{t+\tau}) \quad (1)$$

We are interested in the slow processes. Here,

$$\lambda_i(\tau) = e^{-\kappa_i \tau} \quad (2)$$

are eigenvalues of the propagator that decay exponentially with lag time τ . We order relaxation rates according to $\kappa_1 < \kappa_2 \leq \kappa_3 \leq \dots$ and thus $\lambda_1(\tau) > \lambda_2(\tau) \geq \lambda_3(\tau) \geq \dots$. The first term is special in that it is the only stationary process: $\kappa_1 = 0$, $\lambda_1(\tau) = 1$, $\psi_1(\mathbf{x}) = 1$, thus the first term of the sum is identical to $\mu(\mathbf{x})$. All other terms can be assigned a finite relaxation rate κ_i , or a corresponding relaxation timescale $t_i = \kappa_i^{-1}$, which are quantities of our interest. The eigenfunctions ψ_i are independent of τ and determine the structure of the relaxation process occurring with rate κ_i . The sign structure of $\psi_i(\mathbf{x})$ determines between which substates the corresponding relaxation process is switching and is thus useful for identifying metastable sets, i.e. sets of states that are long-living and interconvert only by rare events [24, 27]. The eigenfunctions are chosen to obey the normalization conditions

$$\langle \psi_i, \psi_j \rangle_\mu = \int d\mathbf{x} \psi_i(\mathbf{x}) \psi_j(\mathbf{x}) \mu(\mathbf{x}) = \delta_{ij}. \quad (3)$$

At a given timescale τ of interest, fast processes with $\kappa \gg \tau^{-1}$ (and correspondingly $t_i \ll \tau$) will have effectively vanished and we are typically left with relatively few slowly-relaxing processes.

Finally, we define the correlation density $c_\tau(\mathbf{x}_t, \mathbf{x}_{t+\tau})$, i.e. the joint probability density of finding the system at \mathbf{x}_t at time t and at $\mathbf{x}_{t+\tau}$ at time $t + \tau$:

$$c_\tau(\mathbf{x}_t, \mathbf{x}_{t+\tau}) = \mu(\mathbf{x}_t) p_\tau(\mathbf{x}_t, \mathbf{x}_{t+\tau}) \quad (4)$$

Observed dynamics and rate theory

Let us consider the case that we are only interested in a single relaxation process – the slowest. Below, we sketch a rate theory for this case. Details of the derivation can be found in the *Supplementary Information*. Based on

the definitions above, the correlation density can then be written as:

$$\begin{aligned} c_\tau(\mathbf{x}_t, \mathbf{x}_{t+\tau}) &= \mu(\mathbf{x}_t)\mu(\mathbf{x}_{t+\tau}) \\ &\quad + e^{-\kappa_2\tau} \mu(\mathbf{x}_t)\psi_2(\mathbf{x}_t)\mu(\mathbf{x}_{t+\tau})\psi_2(\mathbf{x}_{t+\tau}) \\ &\quad + e^{-\kappa_3\tau} \mu(\mathbf{x}_t)p_{\tau,\text{fast}}(\mathbf{x}_t, \mathbf{x}_{t+\tau}) \end{aligned} \quad (5)$$

with

$$p_{\tau,\text{fast}}(\mathbf{x}_t, \mathbf{x}_{t+\tau}) = \sum_{i=3}^{\infty} e^{-(\kappa_i - \kappa_3)\tau} \psi_i(\mathbf{x}_t)\mu(\mathbf{x}_{t+\tau})\psi_i(\mathbf{x}_{t+\tau}) \quad (6)$$

subsuming the fast processes.

Exact rate: The exact rate of interest κ_2 can be recovered as follows: If we know the exact corresponding eigenfunction $\psi_2(\mathbf{x})$, it follows from Eq. (1) and (3) that its autocorrelation function evaluates to:

$$\begin{aligned} \lambda_2(\tau) &= \langle \psi_2(0)\psi_2(\tau) \rangle \\ &= \iint d\mathbf{x}_t d\mathbf{x}_{t+\tau} c_\tau(\mathbf{x}_t, \mathbf{x}_{t+\tau}) \psi_2(\mathbf{x}_t) \psi_2(\mathbf{x}_{t+\tau}) \\ &= e^{-\kappa_2\tau} \end{aligned} \quad (7)$$

where $\langle \cdot \rangle$ denotes the time average, that is here identical to the ensemble average due to ergodicity of the dynamics. $\langle \psi_2(0)\psi_2(\tau) \rangle$ yields the exact eigenvalue $\lambda_2(\tau)$ and thus also an exact rate estimate of $\hat{\kappa}_2 = -\tau^{-1} \ln \lambda_2(\tau) = \kappa_2$, independently of the choice of τ .

Projected dynamics: We may only observe a (possibly poor) order parameter $y(\mathbf{x}) : \Omega \rightarrow \mathbb{R}$ upon which the high-dimensional dynamics is projected. When histogramming the observed dynamics in y , this histogram will, for sufficient statistics, approximate the stationary probability density projected onto y :

$$\mu_y(y') = \int d\mathbf{x} \delta(y' - y(\mathbf{x}))\mu(\mathbf{x}) \quad (8)$$

Since the observer has only information about the dynamics in y available, the eigenfunction ψ_2 is not accessible as it is defined in the whole state space Ω . Thus, it is not possible to calculate the autocorrelation function of ψ_2 exactly and Eq. (7) cannot be used to estimate the rate κ_2 . At best, we have an approximate model function $\tilde{\psi}_2(y(\mathbf{x}))$, which we require to be normalized by

$$\langle \tilde{\psi}_2, 1 \rangle_\mu = 0, \quad \langle \tilde{\psi}_2, \tilde{\psi}_2 \rangle_\mu = 1. \quad (9)$$

$\tilde{\psi}_2$ approximates the true eigenfunction ψ_2 that is a function of full phase space \mathbf{x} only as a function of y :

$$\begin{aligned} \tilde{\psi}_2(y(\mathbf{x})) &= \langle \tilde{\psi}_2, \psi_2 \rangle_\mu \psi_2 + \sum_{i>2} \langle \tilde{\psi}_2, \psi_i \rangle_\mu \psi_i \\ &= \sqrt{\alpha} \psi_2(\mathbf{x}) + \epsilon(\mathbf{x}), \end{aligned} \quad (10)$$

where the true eigenfunction ψ_2 enters with coefficient $\sqrt{\alpha} = \langle \psi_2, \psi_2 \rangle_\mu$ while the remaining eigenfunctions contribute to the error $\epsilon(\mathbf{x})$. The autocorrelation function of $\tilde{\psi}_2$, which we denote as $\langle \tilde{\psi}_2(0)\tilde{\psi}_2(\tau) \rangle = \langle \tilde{\psi}_2(y(\mathbf{x}_t))\tilde{\psi}_2(y(\mathbf{x}_{t+\tau})) \rangle$, now evaluates to [19]

$$\begin{aligned} \tilde{\lambda}_2(\tau) &= \langle \tilde{\psi}_2(0)\tilde{\psi}_2(\tau) \rangle \\ &= \alpha e^{-\kappa_2\tau} + \sum_{i>2} \langle \psi_i, \tilde{\psi}_2 \rangle_\mu^2 e^{-\kappa_i\tau} \end{aligned} \quad (11)$$

where

$$\alpha = \langle \psi_2, \tilde{\psi}_2 \rangle_\mu^2.$$

This autocorrelation function does not yield the exact eigenvalue $\lambda_2(\tau)$, but some approximation $\tilde{\lambda}_2(\tau)$. For $\tau \gg \kappa_3^{-1}$, which can readily be achieved for clear two-state processes where $\kappa_2 \gg \kappa_3$, the sum on the right hand side disappears:

$$\tilde{\lambda}_2(\tau) \approx \alpha e^{-\kappa_2\tau}. \quad (12)$$

This suggests that the true rate, as well as a measure of reaction coordinate quality, could be recovered from large tau decay of an appropriately good trial function even from the projected process. We elaborate this concept in subsequent sections. In experiments, the relaxation rates κ_2, κ_3 , etc, are initially unknown and hence the validity of Eq. (12) can only be checked a posteriori, e.g. by the fact that estimates based upon Eq. (12) are independent of the lag time τ .

Existing rate estimators

Many commonly used rate estimators consist of two steps: (1) they (explicitly or implicitly) calculate an autocorrelation function $\tilde{\lambda}_2(\tau)$ of some function $\tilde{\psi}_2$, and (2) transform $\tilde{\lambda}_2(\tau)$ into a rate estimate $\tilde{\kappa}_2$. In order to derive an optimal estimator, it is important to understand how the systematic error of the estimated rate on each of the two steps. Please refer to the SI for a derivation of the subsequent results.

Many rate estimators operate by defining a single dividing surface which splits the state space into reactants A and products B . Calling $h_A(y)$ the indicator function which is 1 for set A and 0 for set B , one may define the normalized fluctuation autocorrelation function of state A [22]

$$\tilde{\lambda}_2(t) = \frac{\langle h_A(0)h_A(\tau) \rangle - \langle h_A \rangle^2}{\langle h_A^2 \rangle - \langle h_A \rangle^2} = \langle \tilde{\psi}_2(0)\tilde{\psi}_2(\tau) \rangle \quad (13)$$

that can also be interpreted as an autocorrelation function $\tilde{\lambda}_2(t)$ with a step function $\tilde{\psi}_{2,\text{divide}}(y) = (h_A(y) - \pi_A)/\sqrt{\pi_A\pi_B}$. Here, $\pi_A = \langle h_A \rangle_\mu$ is the stationary probability of state A and $\pi_B = 1 - \pi_A$ the stationary probability of state B . Other rate estimates choose $\tilde{\psi}_2$ to be the

signal $y(t)$ itself or the committor function between two pre-defined subsets of the y coordinate [28]. We show that none of these choices is optimal, and the optimal choice of $\tilde{\psi}_2$ will be derived in the subsequent section.

Existing rate estimators largely differ by step (2), i.e. how they transform $\tilde{\lambda}_2(t)$ into a rate estimate $\tilde{\kappa}_2$. This procedure then determines the functional form of the systematic estimation error. We subsequently list bounds for these errors (see SI for derivation).

Reactive flux rate. Chandler, Montgomery and Berne [3, 17] considered the reactive flux correlation function as a rate estimator: $\tilde{\kappa}_{2,\text{rf}}(\tau) = -\frac{d}{dt}\tilde{\lambda}_2(\tau)$. Its error is

$$\tilde{\kappa}_{2,\text{rf}} - \kappa_2 = \kappa_2(\alpha - 1) + \sum_{i>2} \langle \tilde{\psi}_2, \psi_i \rangle_\mu^2 \kappa_2 e^{-\kappa_i \tau} > 0 \quad (14)$$

which becomes 0 for a perfect reaction coordinate (i.e. a perfect choice of $\tilde{\psi}_2 = \psi_2$ that leads to $\alpha = 1$) but can be very large otherwise.

Transition state theory rate. The transition state theory rate, which measures the instantaneous flux across the dividing surface between A and B , can be computed from the short-time limit of the reactive flux [3], $\hat{\kappa}_{2,\text{tst}} = \lim_{\tau \rightarrow 0^+} \tilde{\kappa}_{2,\text{rf}}(\tau)$ such that the error in the is given by

$$\tilde{\kappa}_{2,\text{tst}} - \kappa_2 = \kappa_2(\alpha - 1) + \sum_{i>2} \langle \tilde{\psi}_2, \psi_i \rangle_\mu^2 \kappa_2 > \tilde{\kappa}_{2,\text{rf}} - \kappa_2 \quad (15)$$

which is always an overestimate of the true rate and the reaction flux rate.

Integrating the correlation function. Another means of estimating the rate is via the integral of the correlation function, $\tilde{\kappa}_{2,\text{int}} = -\left(\int_0^\infty d\tau \tilde{\lambda}_2(\tau)\right)^{-1}$ (see, e.g., Equation 3.6 of [3]), with the error:

$$\tilde{\kappa}_{2,\text{int}} - \kappa_2 = \kappa_2 \left(\frac{1 - \alpha + \sum_{i>2} \langle \psi_i, \tilde{\psi}_2 \rangle_\mu^2 \frac{\kappa_2}{\kappa_i}}{\alpha + \sum_{i>2} \langle \psi_i, \tilde{\psi}_2 \rangle_\mu^2 \frac{\kappa_2}{\kappa_i}} \right)$$

in the special case that $\kappa_3 \gg \kappa_2$ (time scale separation), the error is approximately given by $\kappa_2(1 - \alpha)/\alpha$. Thus, the error of this estimator becomes zero for the ideal case of an ideal reaction coordinate ($\alpha = 1$), but may be very huge if the reaction coordinate is poor ($\alpha < 1$).

Single- τ rate estimators: A simple rate estimator is to take the value of the autocorrelation function of some function $\tilde{\psi}_2$ at a single value of τ , and transform it into a rate estimate by virtue of Eq. (12). We call these estimators *single- τ estimators*. Ignoring statistical uncertainties, they yield a rate estimate of the form

$$\tilde{\kappa}_{2,\text{single}} = -\frac{\ln \tilde{\lambda}_2(\tau)}{\tau} \quad (16)$$

Quantitatively, the error can be bounded by the expression (see *Supplementary Information*):

$$\tilde{\kappa}_{2,\text{single}} - \kappa_2 \leq -\frac{\ln \alpha}{\tau}. \quad (17)$$

The error becomes identical to this bound for systems with a strong timescale separation, $\kappa_3 \gg \kappa_2$. Eq. (17) decays relatively slowly in time (with τ^{-1} . See Fig. 1 for a two-state example). It will be shown below that methods that estimate rates from counting the number of transitions across a dividing surface, such as Markov state models, are single- τ estimators and are thus subject to the error given by Eq. (17).

The systematic error of single- τ estimators results from the fact that Eq. (16) effectively attempts to fit the tail of a multiexponential decay $\tilde{\lambda}_2(\tau)$ by a single-exponential with the constraint $\tilde{\lambda}_2(0) = 1$. Unfortunately, the ability to improve these estimators by simply increasing τ is limited because the statistical uncertainty of estimating Eq. 12 quickly grows in τ [33].

Multi- τ rate estimators: To avoid the error given by Eq. (17), it is advisable to estimate the rate by evaluating the autocorrelation function $\tilde{\lambda}_2(\tau)$ at multiple values of τ . This can be done e.g. by performing an exponential fit to the *tail* of the $\tilde{\lambda}_2(\tau)$, thus avoiding the constraint $\tilde{\lambda}_2(0) = 1$ [29, 32]. The estimation error $\hat{\kappa}_2 - \kappa_2$ has the form

$$\hat{\kappa}_{2,\text{mult}} - \kappa_2 < c \frac{1 - \alpha}{\alpha} e^{-\tau_1(\kappa_3 - \kappa_2)} \quad (18)$$

where τ_1 is the first lag time from the series (τ_1, \dots, τ_m) used for fitting, and the constant c also depends on the lag times and the fitting algorithm used. The *Supplementary Information* shows that for several fitting algorithms, such as a least-squares procedure at the time points $(\tau, 2\tau, \dots, m\tau)$, c is such that

$$\hat{\kappa}_{2,\text{mult}} \leq \tilde{\kappa}_{2,\text{single}}. \quad (19)$$

Thus, the multi- τ estimator always is always better than the single- τ estimator (see SI). The main advantage of multi- τ estimators is that their convergence rate is exponential in τ when the time scale separation $\kappa_3 - \kappa_2$ is not vanishing (compare to Eq. 17). Thus, multi- τ estimators are better the larger the timescale separation between the slowest and the other relaxation rates in the system is. Note that the systematic error of a multi- τ estimate thus decays much faster in τ than its statistical error that decays by τ^{-1} [33].

In the absence of statistical error, all of the above rate estimation methods yield an overestimation of the rate, $\tilde{\kappa}_2 \geq \kappa_2$.

Best reaction coordinate - optimal choice of $\tilde{\psi}_2$

It was shown above that multi- τ estimators are the best choice for converting an autocorrelation function

into a rate estimate. However, what is the best possible choice $\hat{\psi}_2 = \tilde{\psi}_{2,\text{optimal}}$ given that only a specified order parameter y is observable? In other words, which function should the observed dynamics be projected upon in order to obtain an optimal rate estimator? Following Eq. (16), the optimal choice $\hat{\psi}_2$ is the one which maximizes the parameter α , as this will minimize the systematic error from a direct rate estimation by virtue of Eq. (17), and also minimize the systematic error involved in estimating κ_2 from an exponential fit to Eq. (12). We are thus seeking the solution of:

$$\hat{\psi}_2 = \arg \max_{\tilde{\psi}_2} \alpha = \arg \max_{\tilde{\psi}_2} \tilde{\lambda}_2(\tau) \quad (20)$$

subject to the normalization Eq. (9). Here, $\arg \max_{\tilde{\psi}_2} \alpha$ denotes the function that maximizes α over the space of functions $\tilde{\psi}_2(y)$. For a sufficiently large set of n basis functions, $\gamma(y) = (\gamma_1(y), \dots, \gamma_n(y))$, the optimal eigenfunction approximant $\hat{\psi}_2$ is approximated by a linear combination $\hat{\psi}_2(y) \approx \sum_{i=1}^n c_i \gamma_i(y)$ with coefficients $\mathbf{c} = (c_1, \dots, c_n)$. When $\gamma(y)$ is chosen to be an orthogonal basis set, then $\hat{\psi}_2 = \arg \max_{\tilde{\psi}_2} \alpha$ can be approximated by the Ritz method [19, 25]. An easy way to do this approximation in practice is to perform a fine discretization of y by histogram windows. Using a binning with bin boundaries y_1, \dots, y_{n+1} , and the corresponding indicator functions $\gamma_i = h_{[y_i, y_{i+1}]}$, then the above optimization problem is solved by estimating the transition probability matrix with elements

$$T_{ij} = \mathbb{P}(y(\tau) \in [y_j, y_{j+1}] \mid y(0) \in [y_i, y_{i+1}]) \quad (21)$$

and calculating \mathbf{c} as the second eigenvector:

$$\mathbf{T}\mathbf{c} = \lambda_2 \mathbf{c} \quad (22)$$

where $\lambda_2 < 1$ is the second-largest eigenvalue of \mathbf{T} . Note that a given optimal $\hat{\psi}_2(y)$ can still be used with single- τ and multi- τ rate estimators that would produce different estimates for κ_2 .

Reaction coordinate quality (RCQ)

Evaluating how well a given putative reaction coordinate captures complex dynamical behavior is of great general interest. Previous studies have proposed ways to measure the reaction coordinate quality (RCQ) that are based on comparing the observed dynamics to specific dynamical models or testing the ability of the observable to model the committor or splitting probability between two chosen end-states A and B [23]. These metrics are either only valid for specific models of dynamics or themselves require a sufficiently good separation of A and B by definition, restricting their applicability to observables with rather good RCQs.

The pre-factor α in Eq. (12) is a measure between 0 and 1 quantifying how good a reaction coordinate the model $\psi_2(y)$ is, and by virtue of Eqs. (17) and (18) how large the error in our rate estimate can be. The RCQ α can be estimated by an exponential fit to the autocorrelation function Eq. (12) of the model function $\tilde{\psi}_2(y)$ employed. For the optimal choice $\hat{\psi}_2 = \tilde{\psi}_2$ (Eq. (20)), we denote this prefactor $\hat{\alpha}$, where $\hat{\alpha} = \alpha(\hat{\psi}_2) \geq \alpha(\tilde{\psi}_2)$, i.e. $\hat{\alpha}$ is the best possible (maximal) RCQ of the observable used. Thus, we propose $\hat{\alpha}$ as a general measure for the quality of the reaction coordinate. This RCQ is as general as possible, as it makes no assumptions about the class of dynamics in the observed coordinate, and does not depend on any subjective choices such as the choice of two reaction end-states A and B in terms of the observable y . Through the derivation above it has also been shown that $\hat{\alpha}$ measures the fraction of amplitude by which the slowest process is observable, which is exactly the property one would expect from a measure of the RCQ: $\hat{\alpha}$ is 1 for a perfect reaction coordinate and 0 if the slowest process is exactly orthogonal to the observable.

Finally, $\hat{\alpha}$ can be determined by the spectral estimation procedure described below. Figures 1 and 2 show estimates of the RCQ α of different projected dynamics using different rate estimators.

Markov (state) models (MSMs)

MSMs have recently gained popularity in the modeling of stochastic dynamics from molecular simulations [4, 21, 24, 30, 31]. MSMs can be understood as a way of implicitly performing rate estimates via discretizing state space into small substates. Let us consider a MSM obtained by finely discretizing the observed space y into bins and estimating a transition matrix $\mathbf{T}(\tau)$ amongst these bins. We have seen that this procedure approximately solves the optimization problem of Eq. (20) and the leading eigenvector of $\mathbf{T}(\tau)$ approximates the best possible reaction coordinate, $\hat{\psi}_2(y)$, available for the given observable y . Ref [30] has suggested to use the implied timescale $\hat{t}_2 = -\tau / \ln(\hat{\lambda}_2(\tau))$ as an estimate for the system's slowest relaxation timescale, and at the same time for a test which choice of τ leads to a MSM with a small approximation error. These implied timescales correspond to the inverse relaxation rates and therefore the MSM rate estimate is described by Eq. (16) with the choice $\tilde{\psi}_2 = \hat{\psi}_2$. A sufficiently fine MSM thus serves as an optimal single- τ rate estimator as it uses the maximum RCQ $\hat{\alpha}$ for observables that are being discretized. However, when these observables have a poor RCQ $\hat{\alpha}$ since they are poorly separating the slowly-converting states, there is a substantial rate estimator error according to Eq. (17) that decays slowly with τ^{-1} . This explains the

slow convergence of implied timescales shown in recent MSM studies [1, 4, 20, 24, 30].

Spectral estimation

The optimal estimator for κ_2 is thus one that fits the exponential decay of κ_2 while minimizing the fitting error Eq. (18). As analyzed above, the systematic fitting error is minimized by any multi- τ estimator. In order to obtain a numerically robust fit, especially in the case when statistical noise is present, it is optimal to fit to an autocorrelation function $\hat{\lambda}_2(\tau)$ where the relevant slowest decay has maximum amplitude α . This is approximately achieved by constructing a fine discretization MSM on the observed coordinate (see Section “Best reaction coordinate”). Thus, the optimal estimator of κ_2 proceeds as follows:

1. Obtain a fine discretization of the observed coordinate y into n bins, say $[y_i, y_{i+1}]$ for $i \in 1 \dots n$.
2. Construct a row-stochastic transition matrix $\mathbf{T}(\tau)$ for different values of τ . The estimation of transition matrices from data have been described in detail [24]. A simple way of estimating $\mathbf{T}(\tau)$ is the following: (i) for all pairs i, j of bins, let $c_{ij}(\tau)$ be the number of times the trajectory has been in bin i at time t and in bin j at time $t + \tau$, summed over all time origins t ; (ii) estimate the elements of $\mathbf{T}(\tau)$ by $T_{ij}(\tau) = c_{ij}(\tau) / \sum_k c_{ik}(\tau)$. A numerically superior approach is to use a reversible transition matrix estimator [24].
3. Calculate the discrete stationary probability $\boldsymbol{\mu}$ and the discrete eigenvector $\hat{\boldsymbol{\psi}}_2$ by solving the eigenvalue equations:

$$\mathbf{T}^T(\tau)\boldsymbol{\mu} = \boldsymbol{\mu} \quad (23)$$

$$\mathbf{T}(\tau)\hat{\boldsymbol{\psi}}_2 = \hat{\lambda}_2\hat{\boldsymbol{\psi}}_2 \quad (24)$$

with the largest eigenvalues $\lambda_1 = 1 < \hat{\lambda}_2 \leq \hat{\lambda}_3$. \mathbf{T}^T denotes the transpose of the transition matrix. The i th element of the vectors $\boldsymbol{\mu}$ and $\hat{\boldsymbol{\psi}}_2$ approximate the stationary density $\mu(y)$ and $\hat{\psi}_2$ on the respective point $y = \frac{y_i + y_{i+1}}{2}$. Functions $\hat{\mu}(y)$ and $\hat{\psi}_2(y)$ can be obtained by some interpolation method.

4. Estimate $\hat{\kappa}_2$ and $\hat{\alpha}$ via an exponential fit of $\alpha e^{-\kappa_2 \tau}$ to the tail of $\hat{\lambda}_2(\tau) = \langle \hat{\psi}_2(t)\hat{\psi}_2(t + \tau) \rangle_t$.

Note that this estimator is optimal in terms of minimizing the systematic error. When dealing with real data, the amount of statistics may set restrictions of how fine a discretization is suitable and how large a lag time τ will yield reasonable signal to noise. This issue is discussed in various other contributions [33].

In order to partition the estimated relaxation rate $\hat{\kappa}_2$ to microscopic transition rates \hat{k}_{AB} , \hat{k}_{BA} (for the $A \rightarrow B$ and $B \rightarrow A$ transitions, respectively), we need to define states A and B , i.e. split state space into two subsets A and B . We have seen above that any choice of a single dividing surface will deteriorate the eigenfunction $\hat{\psi}_2$ and thus be a suboptimal choice for A and B . PCCA theory [8, 14] tells us that there is a way of splitting state space into substates and at the same time maintain optimal approximations to the exact eigenfunctions (here ψ_2): The state assignment must be fuzzy, i.e. instead of choosing dividing surfaces that uniquely assign points x to either A or B , we have fuzzy membership functions $\chi_A(x)$ and $\chi_B(x)$ with the property $\chi_A(x) + \chi_B(x) = 1$. These membership functions can be calculated after ψ_2 is known. Following the derivation given in the appendix, they turn out to be:

$$\hat{\chi}_{A,i} = \frac{\max \hat{\psi}_2 - \hat{\psi}_{2,i}}{\max \hat{\psi}_2 - \min \hat{\psi}_2} \quad (25)$$

$$\hat{\chi}_{B,i} = \frac{\hat{\psi}_{2,i} - \min \hat{\psi}_2}{\max \hat{\psi}_2 - \min \hat{\psi}_2}. \quad (26)$$

Since we are restricted to the projected eigenfunction $\hat{\psi}_2$, we can determine the optimal choice $\hat{\chi}_A(x)$ and $\hat{\chi}_B(x)$ from $\hat{\psi}_2(x)$. Together with the estimated stationary density $\hat{\mu}(x)$ which can e.g. be obtained by computing a histogram from sufficiently long equilibrium trajectories, the probability density of being in A and B when projected onto the observable y can be calculated:

$$\boldsymbol{\mu}_{A,i} = \hat{\chi}_{A,i}\boldsymbol{\mu}_i \quad (27)$$

$$\boldsymbol{\mu}_{B,i} = \hat{\chi}_{B,i}\boldsymbol{\mu}_i \quad (28)$$

The probability of being in A and B is thus given by:

$$\pi_A = \sum_i \boldsymbol{\mu}_{A,i} \quad (29)$$

$$\pi_B = \sum_i \boldsymbol{\mu}_{B,i} = 1 - \pi_A \quad (30)$$

and these probabilities can be used to split $\hat{\kappa}_2$ into microscopic transition rates \hat{k}_{AB} and \hat{k}_{BA} :

$$\hat{k}_{AB} = \pi_B \hat{\kappa}_2 \quad (31)$$

$$\hat{k}_{BA} = \pi_A \hat{\kappa}_2 \quad (32)$$

Note that the assignment of labels “ A ” and “ B ” to parts of state space is arbitrary. Eq. (31) is the transition rate from A to B as defined by Eqs. (25)-(26), and Eq. (32) is the corresponding transition rate from B to A .

The results of spectral estimation are presented for a two-dimensional diffusion model projected onto different order parameters (Fig. 1) and compared to a multi- τ estimator using a dividing surface and a single- τ MSM estimate. In contrast to the other estimators, the spectral

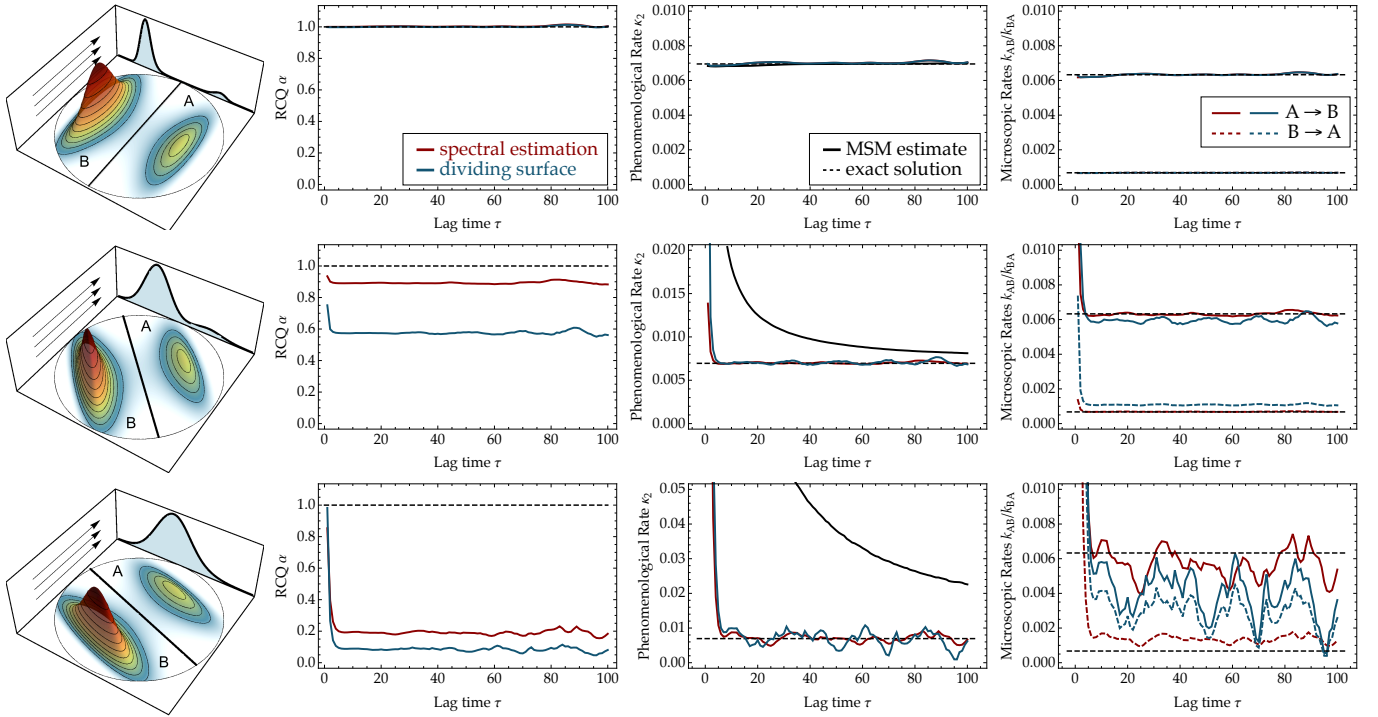


Figure 1: Illustration of the reaction coordinate quality (RCQ) α and different rate estimates using overdamped Langevin dynamics in a two-dimensional two-well potential that is projected onto different observables: perfect projection (first row), intermediate-quality projection (second row), poor projection (third row). For the multi- τ estimators, the lag time τ specifies the start of a time range $[\tau, \tau + 10]$ used for an exponential fit. Column 1: Stationary density of the dynamical model, showing the two populated states in two dimensions and the projected stationary density in the back plane. In the poor projection, both states are indistinguishable in the observed density. Column 2: Estimated RCQ factor α from spectral estimation (red), and from exponential fitting to the number correlation function using a dividing surface at $y = 0$ (blue). With increasing overlap of the slowly-converting states, the RCQ α decreases and the direct MSM rate estimate deteriorates. While the spectral estimator yields an approximation to the true RCQ $\hat{\alpha}$, the α from dividing surfaces is significantly lower in rows 2 and 3. Column 3: Estimated relaxation rate κ_2 using the second eigenvalue of a transition matrix at τ (solid black), using an exponential fit to correlation function at the dividing surface at $y = 0$ (blue), and spectral estimation (red). The black dotted line is the reference solution, obtained from a direct MSM estimate for $\tau = 50$ in row 1. Column 4: The transition rates k_{AB} (dashed) and k_{BA} (solid) calculated using the dividing surface estimate (blue) and from the partial densities of the spectral estimator (red).

estimator yields results that have no or little systematic bias even for very poor reaction coordinates. Moreover, the statistical fluctuations of the spectral estimator are smaller than for the dividing surface estimator. Fig. 2 shows an application of the spectral estimator to real experimental data obtained from an optical tweezer experiment that probes the end-to-end distance fluctuations of the p5ab RNA hairpin. The RCQ α estimates show that the reaction coordinate used here is very good. Yet, the spectral estimation yields results for the transition rates k_{AB} and k_{BA} that are slightly different from the dividing surface estimates.

An overview of the relative performances of three estimators is given in Table I: Markov model, multi- τ fit on a dividing surface-based number correlation function and spectral estimator. This scheme illustrates how these different estimators operate and that the spectral estimator combines ideas from both Markov models and exponential-fitting estimators in order to combine their

strengths.

Conclusions

We have described a rate theory for ergodic and reversible dynamical systems for which only an order parameter that is potentially a poor reaction coordinate is available. Based on the theory, the performance of existing rate estimators could be quantified and compared. For example, the relatively large systematic estimation error in the implied timescales / implied rates of Markov state models is explained. Following the theory, an optimal estimator is proposed that we refer to as *spectral estimator*. The spectral estimator is new in that it provides optimal estimates for three types of quantities:

1. The reaction coordinate quality (RCQ) $\hat{\alpha}$, which is independent of any specific dynamical model and also does not need the definition of an “A” or “B”

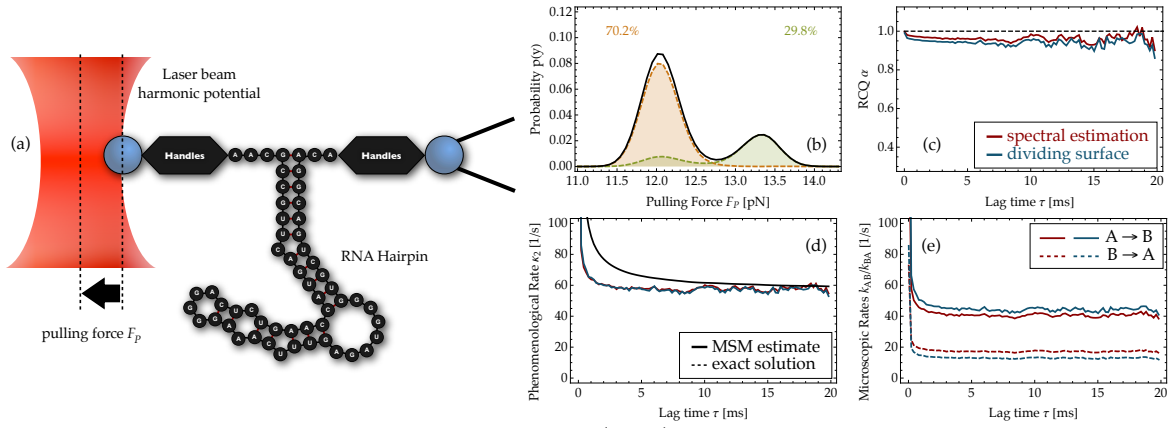


Figure 2: Estimates for rates and the reaction coordinate quality (RCQ) from equilibrium single-molecule force probe experiments on an RNA hairpin. The equilibrium end-to-end fluctuation of the RNA were probed by an optical tweezer [6]. For the multi- τ estimators, the lag time τ specifies the start of a time range $[\tau, \tau + 2.5 \text{ ms}]$ that was used for an exponential fit. Three estimates are compared: The direct MSM estimate (black), a fit to the fluctuation autocorrelation function using a dividing surface at the histogram minimum $y = 12.75 \text{ pN}$ (blue), and spectral estimation (red). (a) schematic experimental setup. (b) the stationary probability of observing a given force value (solid black line). This probability can also be estimated from a by histogramming the measurement values. The partial probabilities of states A (orange) and B (green) obtained by spectral estimation show that there is a small overlap between the states. Notably, part of state A overlaps into state B. (c) the reaction coordinate quality (RCQ) α . The spectral estimator estimates the optimal value to be $\hat{\alpha} \approx 0.96$ at $\tau = 5 \text{ ms}$ while the best possible dividing surface results in $\alpha \approx 0.94$ at $\tau = 5 \text{ ms}$. (d) estimated relaxation rate κ_2 . The MSM estimate is strongly biased and only approaches the true value after $\tau = 20 \text{ ms}$. Both estimators based on exponential fits of the tail of the autocorrelation function (spectral estimator, dividing surface) agree on a rate of $\hat{\kappa}_2 \approx 58 \text{ s}^{-1}$. (e) estimated microscopic transition rates k_{AB} (dotted) and k_{BA} (dashed). The dividing surface estimator obtains rates that differ by 10-20% from the spectral estimate since it cannot correctly assign the probability of state B that is on the “A” side of the dividing surface.

state and bounds the error in rates estimated from a given reaction coordinate.

2. The dominant relaxation rate κ_2 , as well as the microscopic transition rates k_{AB} and k_{BA} , even if A and B strongly overlap in the observable.
3. The local probability densities, and hence projections of the states A and B in the observable, $\mu_A(y)$ and $\mu_B(y)$, as well as their total probabilities, π_A and π_B . This information is also obtained if A and B strongly overlap in the observable.

Other rate estimators that rely on fitting the exponential tail of a time-correlation function calculated from the experimental recorded trajectories can also estimate κ_2 without systematic error. However, the spectral estimator is unique in also being able to estimate k_{AB} , k_{BA} , $\mu_A(y)$, $\mu_B(y)$ and the RCQ in the presence of states that overlap in the observable order parameter.

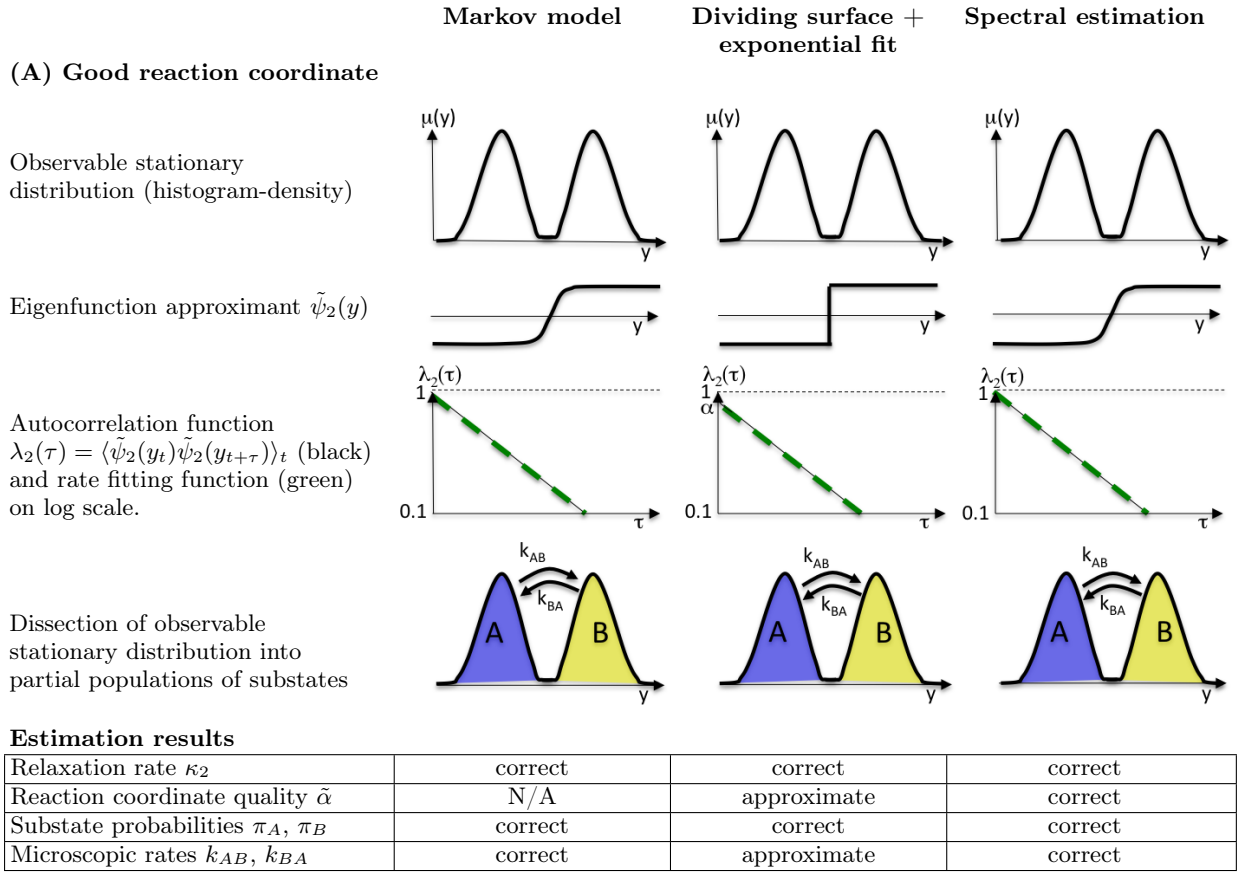
The present study has concentrated on systematic rate estimation errors that are expected in the data-rich regime. We expect that taking the statistical error into consideration will make the spectral estimator described here even more preferable over more direct approaches such as fitting the number autocorrelation function of a dividing surface. This intuition comes from the fact that the spectral estimator maximizes the amplitude α with which the slow relaxation of interest is involved in the autocorrelation function. In the presence of statisti-

cal noise, this will effectively maximize the signal-to-noise ratio and thus lead to an advantage over fitting autocorrelation functions that were obtained differently. However, a systematic treatment of both statistical and systematic error should be made but goes beyond the present study.

The present idea of building an optimal estimator for a single relaxation rate upon the transition matrix estimate of the projected slowest eigenfunction, $\hat{\psi}_2$, is readily extensible to multiple relaxation rates. This lays the basis for a multi-state rate theory for low-dimensional observations of dynamical systems that will be pursued in future studies.

Acknowledgements

The authors thank Susan Marqusee and Phillip J. Elms (UC Berkeley) for sharing the single-molecule force probe data. FN and JHP acknowledge funding from the DFG center MATHEON. JDC acknowledges funding from a QB3-Berkeley Distinguished Postdoctoral Fellowship. We are grateful to Christof Schütte, Attila Szabo, Sergio Bacallado, Vijay Pande and Heidrun Prantel for enlightening discussions and support.



(B) Poor reaction coordinate

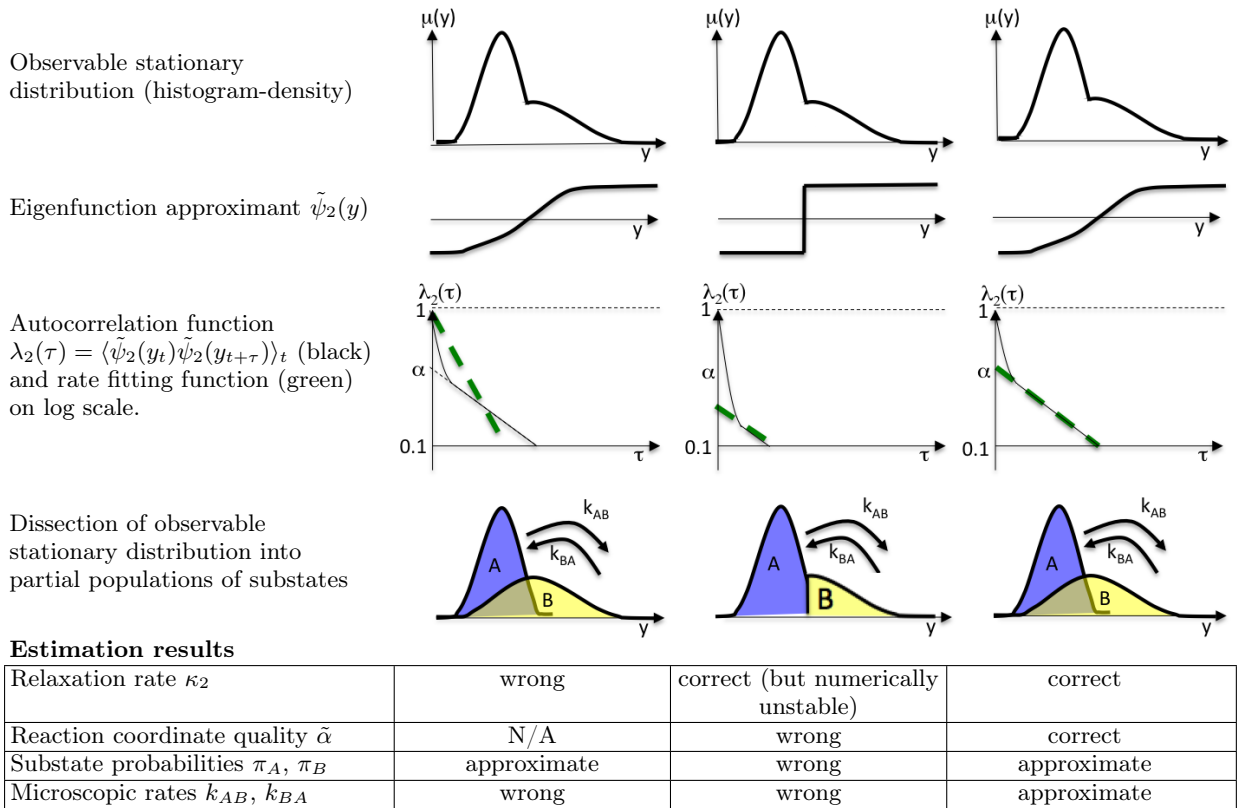


Table I: Scheme comparing spectral estimator (right column) with Markov models constructed from a fine binning along the observable y -coordinate (left column) and an exponential fit to the number correlation function obtained from a dividing surface definition (middle column). Two two-state systems are compared: (A) observed on a nearly perfect reaction coordinate where all three estimators yield the correct rates, yet the spectral estimator is the only one that provides the correct reaction coordinate quality and microscopic rates. (B) observed on a poor reaction coordinate, in which the two substates strongly overlap. Only the spectral estimator can retrieve the correct rates and substate populations.

-
- [1] Gregory R. Bowman, Kyle A. Beauchamp, George Boxer, and Vijay S. Pande. Progress and challenges in the automated construction of Markov state models for full protein systems. *J. Chem. Phys.*, 131(12):124101+, September 2009.
- [2] Nicaolae V. Buchete and Gerhard Hummer. Coarse Master Equations for Peptide Folding Dynamics. *J. Phys. Chem. B*, 112:6057–6069, 2008.
- [3] David Chandler. Statistical mechanics of isomerization dynamics in liquids and the transition state approximation. *The Journal of Chemical Physics*, 68(6):2959–2970, 1978.
- [4] J. D. Chodera, K. A. Dill, N. Singhal, V. S. Pande, W. C. Swope, and J. W. Pitera. Automatic discovery of metastable states for the construction of Markov models of macromolecular conformational dynamics. *J. Chem. Phys.*, 126:155101, 2007.
- [5] J. D. Chodera, W. C. Swope, J. W. Pitera, and K. A. Dill. Long-time protein folding dynamics from short-time molecular dynamics simulations. *Multiscale Model. Simul.*, 5:1214–1226, 2006.
- [6] John D. Chodera, Phillip Elms, Frank Noé, Bettina Keller, Christian M. Kaiser, Aaron Ewall-Wice, Susan Marqusee, Carlos Bustamante, and Nina Singhal Hinrichs. Bayesian hidden markov model analysis of single-molecule force spectroscopy: Characterizing kinetics under measurement uncertainty. <http://arxiv.org/abs/1108.1430>, 2011.
- [7] John D. Chodera, Phillip J. Elms, William C. Swope, Jan-Hendrik Prinz, Susan Marqusee, Carlos Bustamante, Frank Noé, and Vijay S. Pande. A robust approach to estimating rates from time-correlation functions. <http://arxiv.org/abs/1108.2304>, 2011.
- [8] P. Deuffhard and M. Weber. Robust Perron cluster analysis in conformation dynamics. *ZIB Report*, 03-09, 2003.
- [9] Elliot L. Elson and Douglas Magde. Fluorescence Correlation Spectroscopy. I. Conceptual Basis and Theory. *Biopolymers*, 13:1–27, 1974.
- [10] H. Eyring. The activated complex in chemical reactions. *J. Chem. Phys.*, 3:107–115, 1935.
- [11] Irina V. Gopich and Attila Szabo. Decoding the pattern of photon colors in single-molecule FRET. *The journal of physical chemistry. B*, 113(31):10965–10973, August 2009.
- [12] William J. Greenleaf, Michael T. Woodside, and Steven M. Block. High-Resolution, Single-Molecule Measurements of Biomolecular Motion. *Annual Review of Biophysics and Biomolecular Structure*, 36(1):171–190, 2007.
- [13] Bettina Keller, Andreij Y. Kobitski, Uli G. Nienhaus, and Frank Noé. Analysis of single molecule fret trajectories with hidden markov models. *Biophys. J.*, 2011.
- [14] Susanna Kube and Marcus Weber. A coarse graining method for the identification of transition rates between molecular conformations. *J. Chem. Phys.*, 126(2):024103+, 2007.
- [15] Lisa J. Lapidus, William A. Eaton, and James Hofrichter. Measuring the rate of intramolecular contact formation in polypeptides. *Proc. Natl. Acad. Sci. USA*, 97(13):7220–7225, June 2000.
- [16] Sean A. McKinney, Chirlmin Joo, and Taekjip Ha. Analysis of Single-Molecule FRET Trajectories Using Hidden Markov Modeling. *Biophysical Journal*, 91(5):1941–1951, September 2006.
- [17] John A. Montgomery, David Chandler, and Bruce J. Berne. Trajectory analysis of a kinetic theory for isomerization dynamics in condensed phases. *The Journal of Chemical Physics*, 70(9):4056–4066, 1979.
- [18] Frank Noé. Probability Distributions of Molecular Observables computed from Markov Models. *J. Chem. Phys.*, 128:244103, 2008.
- [19] Frank Noé. A variational approach to modeling slow processes in stochastic dynamical systems. *Multiscale Model. Simul.* (submitted, available at: <http://publications.mi.fu-berlin.de/1109/>), 2011.
- [20] Frank Noé, Illia Horenko, Christof Schütte, and Jeremy C. Smith. Hierarchical Analysis of Conformational Dynamics in Biomolecules: Transition Networks of Metastable States. *J. Chem. Phys.*, 126:155102, 2007.
- [21] Frank Noé, Christof Schütte, Eric Vanden-Eijnden, Lothar Reich, and Thomas R. Weikl. Constructing the full ensemble of folding pathways from short off-equilibrium simulations. *Proc. Natl. Acad. Sci. USA*, 106:19011–19016, 2009.
- [22] L. Onsager. Reciprocal relations in irreversible processes II. *Phys. Rev.*, 38:2265–2279, 1931.
- [23] Baron Peters. Using the histogram test to quantify reaction coordinate error. *The Journal of Chemical Physics*, 125(24):241101+, 2006.
- [24] Jan-Hendrik Prinz, Hao Wu, Marco Sarich, Bettina Keller, Martin Fischbach, Martin Held, John D. Chodera, Christof Schütte, and Frank Noé. Markov models of folding kinetics: Generation and validation. *J. Chem. Phys.*, 134:174105, 2011.
- [25] W. Ritz. Über eine neue methode zur lösung gewisser variationsprobleme der mathematischen physik. *J. Reine Angew. Math.*, 135:1–61, 1909.
- [26] Marco Sarich, Frank Noé, and Christof Schütte. On the approximation error of markov state models. *SIAM Multiscale Model. Simul.*, 8:1154–1177, 2010.
- [27] C. Schütte, A. Fischer, W. Huisinga, and P. Deuffhard. A Direct Approach to Conformational Dynamics based on Hybrid Monte Carlo. *J. Comput. Phys.*, 151:146–168, 1999.
- [28] C. Schütte, F. Noé, J. Lu, M. Sarich, and E. Vanden-Eijnden. Markov state models based on milestoning. *J. Chem. Phys.*, 134:204105, 2011.
- [29] James L. Skinner and Peter G. Wolynes. Relaxation processes and chemical kinetics. *J. Chem. Phys.*, 69:2143+, 1978.
- [30] W. C. Swope, J. W. Pitera, and F. Suits. Describing protein folding kinetics by molecular dynamics simulations: 1. Theory. *J. Phys. Chem. B*, 108:6571–6581, 2004.
- [31] Vincent A. Voelz, Gregory R. Bowman, Kyle Beauchamp, and Vijay S. Pande. Molecular Simulation of ab Initio Protein Folding for a Millisecond Folder NTL9. *J. Am. Chem. Soc.*, 132(5):1526–1528, February 2010.
- [32] Huan-Xiang Zhou. Rate theories for biologists. *Quart. Rev. Biophys.*, 43, 2010.
- [33] Robert Zwanzig and Narinder K. Ailawadi. Statistical Error Due to Finite Time Averaging in Computer Experiments. *Physical Review Online Archive (Prola)*, 182:280–283, June 1969.